μ1A deficiency induces a profound increase in MPR300/IGF-II receptor internalization rate

Christoph Meyer[1], Eeva-Liisa Eskelinen[2], Medigeshi Ramarao Guruprasad[1], Kurt von Figura[1] and Peter Schu[1,*]

[1]Zentrum für Biochemie und Molekulare Zellbiologie, Biochemie II, Universität Göttingen, Heinrich-Düker-Weg 12, D-37073 Göttingen, Germany
[2]School of Life Sciences, University of Dundee, Dundee DD1 5EH, Scotland, UK
*Author for correspondence (e-mail: pschu@gwdg.de)

Accepted 13 September 2001
Journal of Cell Science 114, 4469-4476 (2001) © The Company of Biologists Ltd

SUMMARY

The mannose-6-phosphate/IGF-II receptor MPR300 mediates sorting of lysosomal enzymes from the trans-Golgi network to endosomes and endocytosis of hormones, for example, of IGF-II. We analyzed transport of MPR300 in μ1A-adaptin-deficient fibroblasts, which lack a functional AP-1 clathrin adaptor complex. In μ1A-adaptin-deficient fibroblasts, the homologous MPR46 accumulates in endosomes due to a block in retrograde transport to the trans-Golgi network. The MPR300-mediated endocytosis is markedly enhanced. We demonstrate that the seven-fold increase in endocytosis is not associated with an increased steady-state concentration of receptors at the plasma membrane, but with an increased internalization rate of MPR300. Internalization of other receptors that are also endocytosed by AP-2 is not affected. More MPR300 receptors are found in clathrin-coated pits of the plasma membrane, whereas outside coated-areas, more MPR300 are concentrated in clusters and all intracellular receptors reside in endosomes, which are in equilibrium with the plasma membrane. Thus AP-1-mediated transport of MPR300 from endosomes to the TGN controls indirectly the recycling rate of the receptor between the plasma membrane and endosomes.

Key words: AP-1, clathrin, endocytosis, exocytosis, MPR300/IGF-II receptor

INTRODUCTION

The adaptor protein complex 1, AP-1, mediates protein sorting at the trans-Golgi network (TGN). AP-1 consists of four subunits, γ, β1, μ1 and σ1. The μ1-adaptin, as well as the β1-adaptin, interact with sorting motifs in the cytoplasmic tails of transmembrane proteins. The β1, as well as the γ subunit, interact with clathrin to form clathrin-coated transport vesicles (Schmid, 1997; Hirst and Robinson, 1998; Kirchhausen, 1999; Heilker et al., 1999; Doray and Kornfeld, 2001). The μ1-adaptin is present as two isoforms: the ubiquitously expressed μ1A-adaptin and the less widely expressed μ1B-adaptin, which is restricted to polarized epithelial cells (Ohno et al., 1999). We have generated μ1A-adaptin-deficient mice by targeted disruption of the μ1A-adaptin gene and established embryonic fibroblast cell lines. The trimeric γ–β1–σ1-adaptin complex found in these cells, as well as clathrin, do not bind to the TGN, although the TGN remains functional and retains its ability to bind heterotetrameric AP-1 complexes (Meyer et al., 2000).

The cation-dependent mannose-6-phosphate receptor (MPR46) and the cation-independent mannose-6-phosphate/IGF-II receptor (MPR300) are transported by AP-1 at the TGN and by the homologous AP-2 complex at the plasma membrane. They transport different sets of soluble lysosomal enzymes from the TGN to endosomes from where the enzymes reach the lysosome. The receptors are transported back from endosomes to the TGN for another round of transport. Both receptors also appear at the plasma membrane. The mechanisms controlling endosome-to-TGN versus endosome-to-plasma-membrane transport are not known (Kornfeld, 1992; Hille-Rehfeld, 1995). The MPR300 is phosphorylated upon TGN export, and phosphorylation of MPR46 appears to influence endosomal sorting. The importance of these modifications for intracellular sorting are however controversial (Johnson and Kornfeld, 1992; Chen et al., 1993; Hemer et al., 1993; Méresse and Hoflack, 1993; Breuer et al., 1997). MPR46 accumulates in μ1A-deficient cells in EEA1-positive early endosomes, because MPR46 is not transported back to the TGN (Meyer et al., 2000). In control cells, MPR300 and MPR46 are found in the same endosomes, but they appear to be differentially sorted in the endosomes (Klumperman et al., 1993; Meyer et al., 2000). Moreover, MPR300 and MPR46 have different transport functions. Although both receptors are transported to the plasma membrane, leading to 10% located at the cell surface, only the MPR300 is able to bind mannose-6-phosphate (M6P)-carrying proteins and other ligands at the cell surface and to deliver them to endosomes. The MPR300 function critical for development and cell survival is the removal of the insulin-like growth factor IGF-II from the circulation. MPR300-deficient mice are larger than their control litter mates at birth and die perinataly. Mice deficient for both MPR300 and IGF-II are viable (Ludwig et al., 1996; Dittmer et al., 1998). MPR300 also binds to the growth and differentiation factor LIF, retinoic acid and the urokinase receptor, and it is the death receptor for granzyme B of cytotoxic T-cells (Kang et al., 1997; Nykjaer et al., 1998; Blanchard et al., 1999; Motyka et al., 2000). The luminal

domain of MPR300 is composed of 15 homologous repeats, indicating that the receptor is able to endocytose additional, yet unidentified, ligands. The calculated Stokes radius and the ability to bind different ligands simultaneously indicates an elongated conformation of the receptor (York et al., 1999).

In the μ1A-deficient cells, MPR300 mediated endocytosis of ligands is six to seven times higher than in control cells (Meyer et al., 2000). We analyzed the mechanism underlying this strikingly enhanced endocytic capacity by determining MPR300 transport between the plasma membrane and the endosome and vice versa and its distribution within the plasma membrane.

MATERIALS AND METHODS

Cell lines, cell culture, antisera and microscopy

Mouse embryonic fibroblasts were grown in modified DMEM and 10% FCS. MPR300 endocytosis rates were determined in two independently established control and μ1A-deficient cell lines to verify that the difference between cell lines is strictly linked to the genotype. The μ1A-deficient cell line 24 was transfected with μ1A cDNA, which reduced MPR300 endocytosis to control cell levels (data not shown). $39^{+/+}$ and $24^{-/-}$ cell lines were used in this study. Anti-MPR300 antisera were described previously (Meyer et al., 2000). Anti-EEA1 antiserum was a generous gift from H. Stenmark; anti-LBPA was a generous gift from J. Gruenberg; and anti-furin was a generous gift by M. Schäfer. Cy3-labelled mouse transferrin and FITC- and Texas Red-labelled secondary antibodies were from Jackson Immunoresearch. Confocal microscopy was performed using a ZEISS LSM 200 Series equipped with a ZEISS Plan Apochromat 63×/1.40 and Carl Zeiss LSM version 3.95 software. Images were processed for presentation using Adobe Photoshop Version 5 and Deneba Canvas 5.0. Cells were fixed with 3% para-formaldehyde or methanol following standard protocols.

MPR300 biotinylation experiments

MPR300 biotinylation/surface biotinylation

The cells were grown on 3 cm ø culture dishes overnight to about 90% confluency. They were washed 4 × 5 minutes with ice cold biotinylation buffer (10 mM NaP_i pH 8.0; 135 mM NaCl; 10 mM KCl) and incubated on ice with 1 mg/ml sulfo-NHS-SS-biotin (PIERCE) for 3 hours at 4°C in a cold room with temporary agitation. To remove the unbound biotin reagent, the cells were washed 6 × 5 minutes with biotinylation buffer.

Determination of surface MPR300

Surface biotinylated cells were washed, harvested in TIN (0.5% Triton X-100; 50 mM imidazol pH 7; 150 mM NaCl and proteinase inhibitor mix) and homogenized by ultrasonication. Protein concentration was determined with the BIORAD reagent, and 100 μg samples of each clone were frozen until further analysis. Homogenates were centrifuged for 20 minutes at 48,000 ***g***, supernatants were collected and volume equivalents to 300-500 μg total protein were subjected to precepitation with strepavidin-agarose (Pierce) overnight at 4°C. Bound proteins were spun down for 1 minute at 12,000 ***g***, and agarose beads were washed 5 times with PBS/0.1% Triton X-100. Beads and 100 μg of homogenates were boiled in SDS-PAGE sample buffer under non-reducing conditions for 3 minutes and separated on a 5% SDS-gel. After western transfer onto a nitrocellulose membrane (Sartorius) MPR300 was detected with a polyclonal rabbit serum and HRP-coupled secondary antibody. Signals were developed with the chemoluminescent ECL kit (PIERCE), quantified by densitometry (WinCam 2.2 software). Signals obtained from the biotinylated MPR300 were normalized for the protein content.

Internalisation assay

Cells were biotinylated and washed as described. One set of cells was harvested in TIN to measure total cell surface MPR300. Then the cells were incubated for 1 minute at 37°C in DMEM. Cells were cooled by washing with ice cold buffer, and biotin of cell-surface proteins was cleaved off by incubation for 20 minutes with gluthatione solution (600 mg gluthatione; 9 ml 83 mM NaCl, 1 mM $MgCl_2$, 1 mM $CaCl_2$; 300 μl 10 M NaOH; 100 μl 1 M DTT; 1 ml 10% BSA) on ice. As a control, one set of cells was incubated without rewarming. Cells were homogenized in TIN by ultrasonication, incubated for 30 minutes on ice and centrifuged for 20 minutes at 48,000 ***g***. Supernatants were immunoprecipitated with a polyclonal rabbit serum overnight at 4°C. Precipitates were separated on a 5% non-reducing SDS-gel, transfered onto a nitrocellulose membrane and blocked with 1% BSA in PBS/0.2% Tween 20. Biotinylated MPR300 was detected by incubating with streptavidin-HRP (Dianova; 1:5000 in blocking buffer) for 2 hours. Blots were developed with the ECL-kit (PIERCE) and X-ray film exposure. Films were scanned and signals quantified (WinCam 2.2 software).

Recycling assay

Cells were biotinylated and washed as described and loaded with biotinylated receptors by rewarming for 2 minutes in DMEM at 37°C. The biotin of cell-surface proteins was cleaved off as described above, and one set of cells was harvested in TIN. Sequentially, cells were subjected to rewarming/cleaving for 1, 2 or 3 times to measure appearance of internalized receptors at the cell surface. From the cells, MPR300 was extracted and immunoprecipitated as described above.

MPR300 surface labelling and immunoelectron microscopy

Cells were grown on 35 mm culture dishes to subconfluency. The cells were rinsed twice with PBS and then incubated with 3% BSA on ice for 10 minutes. The cell surface was then labelled with rabbit anti-MPR300 (1:200 in 3% BSA/PBS) on ice for 1 hour. The monolayer was washed on ice four times with 1% BSA, and then twice with PBS, before being fixed in 4% para-formaldehyde on ice for 15 minutes. After washing in PBS and quenching in 0.12% glycine, the bound anti-MPR300 was detected with goat F(ab)2 anti-rabbit IgG 10 nm gold (British BioCell, Cardiff). Finally, the cells were washed in PBS-BSA and PBS, fixed in 1% glutaraldehyde, scraped off the dish, pelleted, postfixed in 1% osmium tetroxide and embedded in Epon. Cell-surface labelling was quantitated from 80 nm thin sections by counting gold particles under the electron microscope. The length of membrane on section was measured by intersection counting (Griffiths, 1993). Statistical significance was tested by applying the Mann-Whitney U-test. It is a non-parametric test, which does not request a normal distribution of the measurement results. p-values below 0.05 indicate statistical significance, and this increases with values smaller then 0.01 and 0.001.

LDL and EGF-R degradation

LDL endocytosis and degradation

Cells were grown in DMEM with 5% FCS in 3 cm ø dishes. The medium was replaced by DMEM with 5% LDL free human serum and cultures were incubated for an additional 24 hours. Purified huLDL was labelled with ^{125}I by the iodine monochloride method to 300 cpm/ng. 300.000 cpm/dish of ^{125}I-labeled huLDL was added to the cultures, and cells were incubated for an additional 24 hours. The accumulated non-TCA-precipitable radioactivity in the cells and media was determined by liquid scintillation counting. Background LDL decay was determined by incubating labelled huLDL-containing medium in the absence of cells (Goldstein et al., 1983).

EGF-R endocytosis and degradation

Cells were grown to confluency in 6 cm dishes, serum starved for 1 hour in DMEM, 1% BSA, 20 mM HEPES pH 7.4, and

downregulation was induced by the addition of 500 ng/ml EGF (Santa Cruz Biotechnology Inc.). Cells were washed with PBS, scraped off the plates and protein extracts were prepared. 30 μg of proteins were resolved on 5% SDS-PAGE and blotted onto nitrocellulose membranes. Western blots were developed with rabbit anti-EGF-R serum (Santa Cruz Biotechnology Inc.) and mouse monoclonal anti-α-adaptin antibodies (BD Transduction Laboratories) as an internal control (Wiley et al., 1991). Quantification was performed as described above.

RESULTS

Increased internalization rate of the MPR300

We previously demonstrated that in μ1A-deficient cells, MPR300 mediates endocytosis of M6P-containing ligands such as synthetic phosphomannan-BSA or the lysosomal enzyme arylsulfatase A (ASA). This increase in endocytosis is not associated with an increase in MPR300 expression levels (Meyer et al., 2000). To understand the basis for the strikingly enhanced internalization, we determined the concentration of MPR300 at the cell surface and the internalization rate of cell-surface-associated MPR300.

To determine the fraction of MPR300 present at the cell surface at steady state, the cells were rapidly cooled to 0°C and cell-surface proteins were biotinylated. The biotinylated proteins were collected with streptavidin-agarose. MPR300 was quantified in the cell extracts and in the streptavidin-bound fraction by western-blot (Fig. 1). To our surprise, despite a seven-fold increase in the internalization rate for MPR300 ligands, we did not detect an increase in the number of receptors at the cell surface. In control cells, 11.5% (±2.3; *n*=3) of total MPR300 was located at the plasma membrane, a value corresponding to data in the literature (Klumperman et al., 1993). In μ1A-deficient cells, the fraction of MPR300 accessible to biotinylation at the plasma membrane was 9.2% (±0.5; *n*=3).

We then determined how fast MPR300 is internalized at the plasma membrane. Cultures were kept on ice and cell-surface receptors were labelled with a cleaveable biotin derivative.

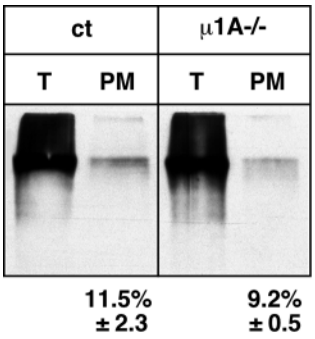

Fig. 1. Surface expression of MPR300 in control (ct) and μ1A-deficient cells (μ1A–/–). Cells were rapidly cooled to 0°C and biotinylated. Biotinylated proteins were precipitated with streptavidin-agarose from 300-500 μg of cell extract proteins. Precipitates of biotinylated proteins and 100 μg of total protein extracts were analyzed in western blots by anti-MPR300 antibodies. Signals were quantified by densitometry and normalized for the protein content (see Materials and Methods for experimental details).

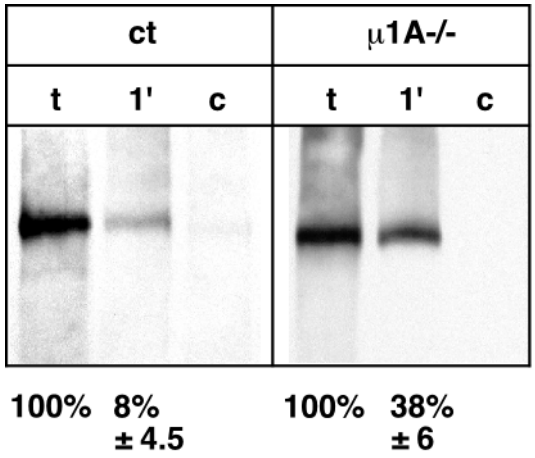

Fig. 2. Internalization rate of MPR300 in control (ct) and μ1A-deficient cells (μ1A–/–). Cell-surface receptors were biotinylated on ice (t), warmed to 37°C for 1 minute and rapidly cooled on ice. Biotin was removed from proteins exposed at the cell surface. MPR300 was immunoprecipitated from cell extracts and precipitates were analyzed by western blots and streptavidin-HRP conjugates. Removal of biotin was quantitative, as indicated by the complete loss of biotinylated MPR300 in cells that were stripped without warming the cultures to 37°C (c).

Afterwards, cultures were warmed to 37°C for 1 minute to allow endocytosis, then cooled on ice to stop transport and to remove biotin at the cell surface by incubation with glutathione. Stripping of biotin was quantitative (Fig. 2). MPR300 was immunoprecipitated from the cell extracts, separated on Laemmli gels and transferred onto nitrocellulose membranes. The biotinylated receptors were detected with streptavidin-HRP conjugates (Fig. 2). Within 1 minute, control cells internalized 8% (*n*=3) of biotinylated receptors, whereas μ1A-deficient cells internalized 38% (*n*=3) of the receptors. These data demonstrate that the enhanced MPR300-mediated endocytosis can largely be explained by an enhanced internalization rate of cell-surface MPR300.

Next we asked whether the internalization rate of other receptors that utilize AP-2 clathrin-coated vesicles for internalization is also increased. For this purpose, we determined low-density-lipoprotein receptor (LDL-R)-mediated LDL endocytosis and degradation and EGF-induced internalization and degradation of the epidermal-growth-factor receptor (EGF-R) (Goldstein et al., 1983; Wiley et al., 1991). LDL-R expression was induced by incubating the cells in LDL-free serum for 24 hours. Cells were incubated for an additional 24 hours in the presence of 300.000 cpm of ^{125}I-LDL. The amount of internalized radioactivity and TCA-soluble radioactivity in the medium were determined (Table 1). μ1A-deficient cells endocytosed 40% less LDL then control cells. The reduction corresponds to 40% lower expression levels of LDL-R in μ1A-deficient cells (not shown). Control and μ1A-deficient cells degraded a comparable fraction (85%) of the LDL that had been internalized (Table 1) during the 24 hour internalization period. This indicates that not only the internalization of LDL, but also its delivery to and degradation within lysosomes is normal in μ1A-deficient cells. Binding of EGF to EGF-R is followed by phosphorylation, AP-2 dependent internalization of the receptor and its delivery to

Table 1. Ligand induced downregulation of EGF-R and LDL uptake and degradation in control (ct) and μ1A-deficient cells (μ1A$^{-/-}$)

A ^{125}I-LDL degradation

	C	M	T
ct	15503±197	92767±2107	108270±2304
μ1A$^{-/-}$	8179±657	55878±2242	64057±2899

B EGF induced EGF-R turnover

	0	30′	90′
ct	100	50	26
μ1A$^{-/-}$	100	57	29

A: LDL-R expression was induced by starving the cells in LDL free serum. 300,000 cpm of ^{125}I-labelled LDL was added to the cultures. After 24 h the amount of radioactivity remaining cell associated after trypsin treatment and the amount of TCA-precipitable radioactivity in the medium was determined. The latter was corrected for TCA-soluble radioactivity in ^{125}I-LDL supplemented medium incubated in the absence of cells. Numbers give the cpm/mg protein of the TCA-soluble radioactivity associated with the cells (C) and in the medium (M).

B: EGF-R endocytosis was induced by the addition of EGF to 0.8 nM. The amount of EGF-R was quantified by western-blot analysis of cell extracts prepared at the indicated time points. Numbers give the amount of EGF-R in percent of time zero.

lysosomes (Wiley et al., 1991; Lamaze and Schmid, 1995). Following incubation in serum-free medium, internalization and degradation of EGF-R was induced by the addition of 500 ng/ml EGF. In control and μ1A-deficient cells, about 50% of the receptors were degraded within 30 minutes (Table 1), indicating that downregulation proceeds in control and μ1A-deficient cells with identical rates. Moreover, fluid phase endocytosis, as measured by horse-radish-peroxidase internalization, is also not effected in μ1A-deficient cells (not shown). These data clearly demonstrate that the increased internalization of MPR300 in μ1A-deficient cells is specific for this receptor and that receptor-mediated and fluid endocytosis proceed at normal rates.

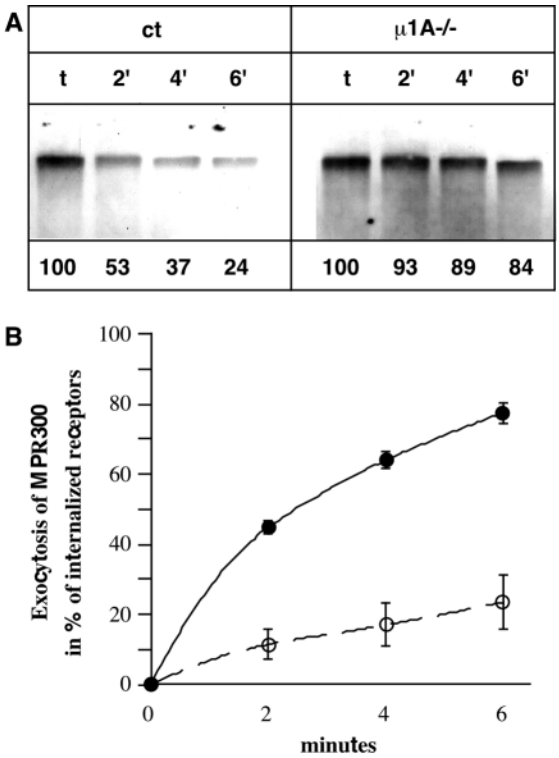

Fig. 3. Exocytosis of internalized MPR300 in control (ct) and μ1A-deficient cells (μ1A–/–). (A) Cells were biotinylated on ice, warmed to 37°C for 2 minutes, cooled on ice and subjected to biotin stripping. The fraction of the internal biotinylated receptors is set to 100% (t). Parallel cultures were subjected to up to three additional cycles of warming to 37°C for two minutes, cooling on ice and biotin stripping. Numbers below give the signal intensities for biotinylated MPR300 as a percentage of the total. (B) Kinetics of exocytosis for biotinylated MPR300, see (A). Numbers correspond to the decrease in intracellular biotinylated receptors. Closed circles and solid line; control cells, open circles; and dashed line, μ1A-deficient cells. Data are from three independent experiments.

Exocytosis of internalized MPR300

Next we determined how fast receptors that had been internalized are transported back to the plasma membrane. Receptors were biotinylated at the plasma membrane at 0°C. The cells were then warmed to 37°C for two minutes to allow endocytosis, again cooled to 0°C, and the receptors remaining at the plasma membrane were de-biotinylated. The fraction of biotinylated receptors internalized within two minutes at 37°C was determined and set to 100% (Fig. 3). Cells in a parallel dish were again warmed to 37°C for 2 minutes, cooled to 0°C and debiotinylated. The decrease of biotinylated receptors during the second warming to 37°C corresponds to the fraction of biotinylated MPR300 that had been re-exported to the cell surface. The cycle of warming to 37°C for 2 minutes and biotin-stripping at 4°C was repeated (Fig. 3). The control cells re-exported within 47% of their internalized biotinylated receptors 2 minutes and 76% within 6 minutes. In μ1A-deficient cells, only 7% of the internalized biotinylated receptors were exported to the cell surface within 2 minutes and 16% within 6 minutes. Thus in μ1A-deficient cells, biotinylated MPR300 reappears at a 6.7 times slower rate at the plasma membrane than in control cells. At steady state, the number of MPR300 that are exported to the cell surface per unit of time must be equal to the number that are internalized per unit of time. As μ1A-deficient cells internalize MPR300 six times faster, this implies that also six times more MPR300 are exported to the cell surface per unit of time. Apparently, the internalized, biotinylated MPR300 is mixed in μ1A-deficient cells with a much larger pool of non-biotinylated MPR300 than in control cells, thus lowering the fraction of biotinylated receptors that is re-exported per unit of time.

The size of this endosomal pool of MPR300 can be calculated from the trafficking rates and from the steady-state distribution of the receptor. As 11.5% of the total MPR300 is at the cell surface (Fig. 1) and is internalized with a rate of 8%/minute (Fig. 2), about 1%/minute of the total MPR300 is transferred from the plasma membrane to endosomes in control cells. Maintenance of steady state requires that also 1%/minute of MPR300 is exported from endosomes to the cell surface. About 25%/minute of biotinylated receptors were found to be exocytosed (Fig. 3). This indicates that they originate from a four times larger pool, which therefore represents 4% of the total MPR300. In μ1A-deficient cells, 9.2% of the total MPR300 is at the plasma membrane and 38% of this is

endocytosed per minute, indicating that about 4%/minute of the total MPR300 become internalized as well as exocytosed to the plasma membrane. Only 4% of the biotinylated MPR300 were found to become exocytosed per minute. Thus, the endosomal pool from which they originate is 25-fold larger than the internalized fraction and must therefore contain essentially all intracellular MPR300 (~90% of total).

MPR300 recycling endosomes

To characterize the endosomes containing MPR300, we performed double-immunofluorescence microscopy for MPR300 and various endosomal markers.

The early endosomal antigen EEA1 interacts with Rab5 and phosphatidylinositol-3-phosphate, facilitating early endosome fusion (Christoforidis et al., 1999). In control cells, we find MPR300/EEA1 colocalization restricted to a few EEA1-positive endosomes (Fig. 4). In μ1A-deficient cells, a large number of EEA1-positive endosomes also contain MPR300. As a measure of colocalization, the yellow spectra of the merged images were quantified. This revealed a 2.3 fold more intense staining in $\mu1A^{-/-}$ cells compared to control cells. We also performed double immunofluorescence with lysobisphosphatidic acid (LBPA), a marker for late endosomes (Kobayashi et al., 1998). We did not observe colocalization of MPR300 with LBPA in control or μ1A-deficient cells (Fig. 4). We also could not detect colocalization with LAMP-1, another marker for late endosomes and lysosomes (Meyer et al., 2000). This demonstrates a redistribution of MPR300 from the TGN to early endosomes.

MPR300 and the transferrin receptor are endocytosed by the same AP-2 CCV, but they are then separated from each other with a half time of 10 minutes (Stoorvogel et al., 1989). Although the transferrin receptor is transported into a recycling endosome from which it is exocytosed, the recycling route of MPR300 back to plasma membrane is not known. To test if MPR300 is redistributed into transferrin receptor recycling endosomes in μ1A-deficient cells, we labelled the recycling endosome by allowing cells to endocytose mouse Cy3-transferrin for 15 minutes. The cells were then fixed and labelled for MPR300 (Fig. 4). In control cells, the majority of vesicles contained either transferrin or MPR300, and colocalization of endocytosed transferrin and MPR300 was limited. μ1A-deficient cells displayed the same distribution of transferrin and MPR300, demonstrating that they are segregated during recycling as in control cells.

The prohormone convertase furin recycles between the TGN and endosomes, and endosomes and the plasma membrane, as MPR300. Transport out of the TGN occurs via AP-1 clathrin-coated vesicles, and the fraction of furin appearing at the cell surface is endocytosed by AP-2 clathrin-coated vesicles (Schäfer et al., 1995; Molloy et al., 1999; Stroh et al., 1999; Teuchert et al., 1999). Available antibodies did not permit us to study colocalization of MPR300 and furin. To detect a redistribution of furin, we performed double-immunofluorescence microscopy for EEA1 and furin. Similar to MPR300, furin is concentrated in the perinuclear region. In μ1A-deficient cells, it is redistributed into peripheral vesicles. In contrast to the MPR300 colocalization with EEA1, furin is not detectable in either cell line (Fig. 4), indicating that the transport pathways of furin and MPR300 are differentially affected by μ1A deficiency.

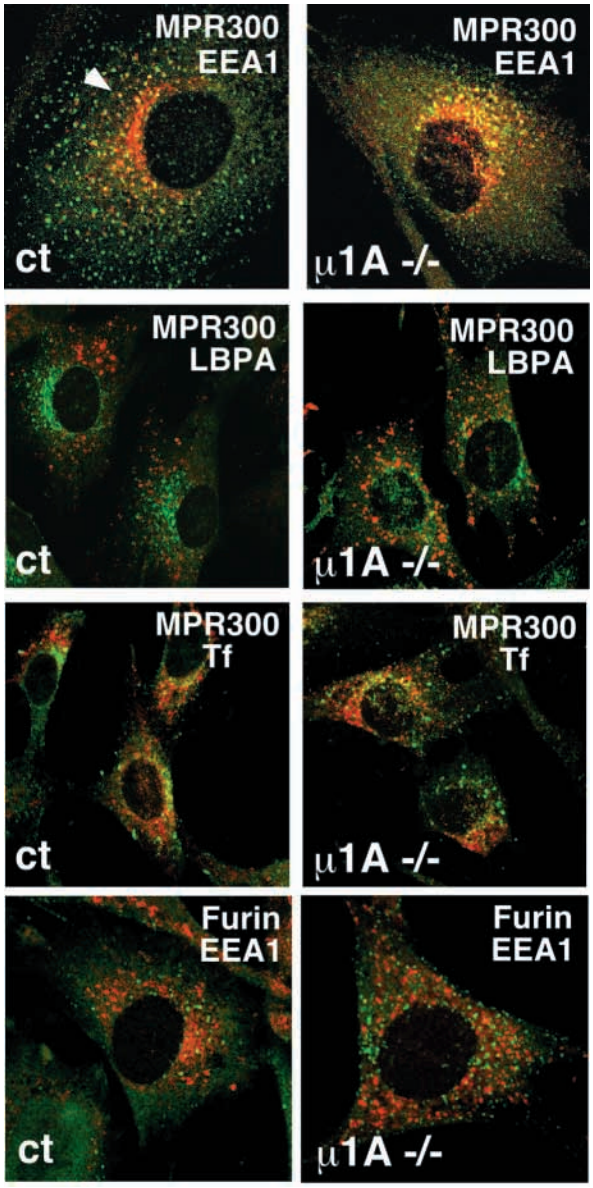

Fig. 4. MPR300-containing endosomes in control (ct) and μ1A-deficient cells (μ1A–/–). Steady-state labeling for MPR300 is shown in red, and the early endosome antigen 1 EEA1 is shown in green. Quantificaton of the yellow spectra revealed a 2.3 fold more intense staining in μ1A–/– cells compared with ct cells. Labelling of late endosomes with LBPA is shown in red and MPR300 is shown in green. Steady-state labelling for MPR300 (green) and Cy3-labelled transferrin (red) is shown endocytosed over 15 minutes. The distribution of EEA1 (green) and furin (red) is also shown.

Distribution of MPR300 in the plasma membrane

To obtain insight into the mechanisms underlying the enhanced internalization rate of MPR300, we compared MPR300 distribution in the plasma membrane of μ1A-deficient and control cells by immunogold staining. Cells were labelled with anti-MPR300 antibodies at 4°C, fixed and processed for immunoelectron microscopy with goat anti-rabbit IgG gold.

In control cells, only 3.95% of coated pits were labelled with gold particles, whereas in μ1A-deficient cells, 17.28% were

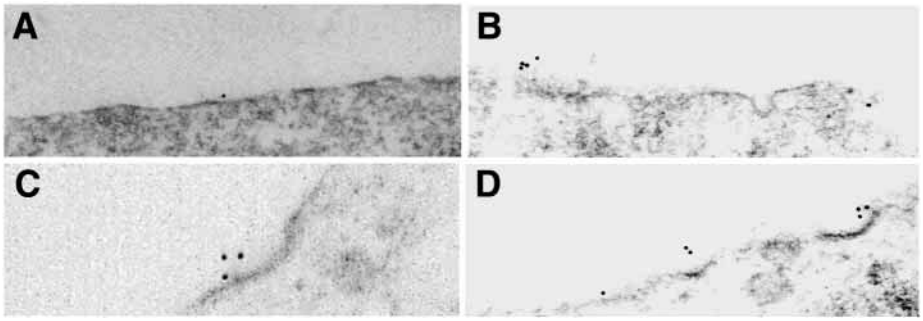

Fig. 5 Immunogold electron microscopy for plasma membrane MPR300. (A) and (B) plasma membrane and coated pit of control cell. (C) and (D) plasma membrane and coated pits of μ1A-deficient cell.

labelled (Table 2; Fig. 5). Coated areas were labelled in both cell lines by 1.4 gold particles on average per cell. When clathrin-coated pits and deeply invaginated coated pits were counted, 22.5% fewer clathrin-coated pits were detected in μ1A-deficient cells, but statistical analysis indicates that this is not significantly different. Taken together, these data indicate that in μ1A-deficient cells, a higher fraction of clathrin-coated pits contain MPR300.

Outside of coated areas, 51.59% of the gold particles were clustered in μ1A-deficient cells, whereas in control cells only 38.24% were clustered.

DISCUSSION

The MPR300 receptor is transported by AP-1 clathrin-coated vesicles from the TGN to endosomes and by AP-2 clathrin-coated vesicles from the plasma membrane to endosomes. From endosomes, it is transported to either the TGN or to the plasma membrane. The mechanisms controlling this sorting event are not known. At steady state, MPR300 is concentrated in the TGN (Kornfeld, 1992; Hille-Rehfeld, 1995). In μ1A-deficient cells, the MPR300/IGF-II receptor is redistributed into peripheral cytoplasmic vesicles and mediates markedly enhanced endocytosis of ligands (Meyer et al., 2000). To understand how AP-1-deficiency enhances MPR300-mediated endocytosis, we analyzed its subcellular distribution and trafficking.

The fraction of MPR300 present at the plasma membrane has been determined in this and other studies to be ~10% (Klumperman et al., 1993). This fraction is not increased in μ1A-deficient cells. The endocytosis rate of the MPR300 receptor however is about five times faster. The increase can account for most, and probably even all, of the seven times higher endocytosis rate observed for MPR300 ligands. The fraction of previously endocytosed receptors that is exocytosed per unit of time was significantly smaller in μ1A-deficient cells. This indicates that the endocytosed receptors mix with a much larger pool of endosomal receptors (Fig. 1; Fig. 2; Fig. 3).

Table 2. Plasma membrane distribution of MPR300

	Gold per cluster outside CP	Proportion of gold in clusters outside CP	Proportion of labelled CP and CV	Gold in CP per μm
Control	1.2692±0.054	38.24±5.6	3.95±0.45	0.00507±0.0009
μ1A$^{-/-}$	1.4654±0.050	51.59±4.1	17.28±5.83	0.01371±0.0034
p-value	0.016*	0.032*	0.004**	0.008*

A total of 347 and 809 gold particles were scored from control and μ1A$^{-/-}$ cells, respectively. A total of 671 and 452 coated pits/vesicles were scored for control and μ1A$^{-/-}$ cells, respectively. In coated pits containing gold, the average number of particles was 1.4 in both cell lines. Coated pits on the plasma membrane and coated vesicles situated at a distance of 200 nm from the plasma membrane were counted. Results are given as mean±s.e.m. between four to six separate estimations. Statistical significance was estimated using a nonparametric Mann-Whitney U-test. p-values below 0.05 indicate statistical significance (asterisks indicate level of statistical significance; see also Materials and Methods).

The size of the endosomal pool of MPR300 that recycles between the plasma membrane was calculated from the trafficking rates and the steady-state distributions to be 4% of the total cellular MPR300. In NRK and HepG2 cells expressing human MPR300, the fraction of MPR300 in early endosomes has previously been determined to be 10%±2.3 by immunogold labelling (Klumperman et al., 1993). In μ1A-deficient cells, 90% of the cellular receptors are localized to endosomes from which they recycle to the plasma membrane. Thus, MPR300 endosome-to-TGN retrograde transport is blocked in the μ1A-deficient cells.

We characterized this endosomal MPR300 pool in μ1A–/– cells by double-immunofluorescence microscopy for MPR300 and endosomal markers. We found extensive colocalization with EEA1, but none with LBPA or LAMP-1. Colocalization with transferrin-containing endosomes is not higher than in control cells, indicating that MPR300 and transferrin receptors are separated along the recycling pathway (Stoorvogel et al., 1989). Future experiments will have to characterize the MPR300-containing endosomes and the recycling pathway of MPR300.

How can the enhanced internalization rate of MPR300 be achieved? It is apparent from the normal internalization rate observed for LDL-R-mediated uptake of LDL-and EGF-triggered delivery of surface EGF-R to lysosomes that the enhanced internalization rate is specific for MPR300, and possibly a few other receptors, but does not reflect a general increase in AP-2 mediated internalization. More MPR300 were found to be clustered outside clathrin-coated pits in μ1A$^{-/-}$ cells compared with control cells. MPR300 itself does not form dimers or homooligomers unlike MPR46. MPR300, however, can be crosslinked by multivalent ligands (York et al., 1999). We can exclude the possibility that ligand-mediated crosslinking contributes to the clustering of MPR300 and its enhanced internalization rate. Treatment of the cells for 2 hours with cycloheximide to clear the biosynthetic pathway from endogenous MPR300 ligands and washing of the cells with

M6P did not affect subsequent endocytosis of arylsulfatase A in the presence of cycloheximide (not shown). Therefore only a minor fraction of cell-surface MPR300 is occupied by endogenous ligands.

At the plasma membrane of μ1A-deficient cells, more MPR300 are concentrated in clusters than in control cells. We propose that a larger fraction of MPR300 arrive at the plasma membrane in a more clustered form. These clusters are likely to be more rapidly integrated into clathrin-coated pits, either due to their diffusion as a raft impairing their rapid lateral diffusion in the plane and/or because they serve directly as nucleation centers for rapid formation of clathrin-coated pits. In μ1A-deficient cells, we found 40% more MPR300 clustered outside coated-pits and 4.4-fold more coated pits and vesicles were labelled in μ1A-deficient cells compared with control cells. In conjunction with the faster internalization rate, this indicates that clustering of MPR300 enhances significantly the rate sy which MPR300 is recruited into coated pits and vesicles.

In the absence of AP-1, MPR300 accumulates in endosomes owing to its impaired return to the TGN. We propose that the higher concentration of MPR300 in endosomes favours clustering of the receptor and increases its exocytosis to the plasma membrane. As discussed above, arrival of clustered receptors at the plasma membrane is thought to accelerate its incorporation into clathrin-coated vesicles to an extent that the steady-state concentration at the plasma membrane is not increased inspite of an increased exocytosis rate of MPR300. Thus AP-1-mediated transport of the MPR300 from endosomes to the TGN indirectly controls, in a negative manner, the trafficking rate of the receptor between the plasma membrane and endosomes and thereby controls MPR300-mediated endocytosis of growth and differentiation factors and lysosomal enzymes.

We thank H. Stenmark (Oslo), J. Gruenberg (Genève) and M. Schäfer (Marburg) for antibodies and E. Wieland (Klinikum Göttingen) for LDL free serum and purified LDL. We also thank C. Hinners for excellent technical assistance and all members of the laboratory for discussions. This work is supported by the Deutsche Forschungsgemeinschaft SFB 523/A6 and the Fonds der Chemischen Industrie.

REFERENCES

Blanchard, F., Duplomb, L., Raher, S., Vusio, P., Hoflack, B., Jacques, Y. and Godard, A. (1999). Mannose 6-Phosphate/Insulin-like growth factor II receptor mediates internalization and degradation of leukemia inhibitory factor but not signal transduction. *J. Biol. Chem.* **274**, 24685-24693.

Breuer, P., Körner, C., Böker, C., Herzog, A., Pohlmann, R. and Braulke, T. (1997). Serine phosphorylation site of the 46-kDa mannose 6-phosphate receptor is required for transport to the plasma membrane in Madin-Darby canine kidney and mouse fibroblast cells. *Mol. Biol. Cell* **8**, 567-576.

Chen, H. J., Remmler, J., Delaney, J. C., Messner, D. J. and Lobel, P. (1993). Mutational analysis of the cation-independent mannose 6-phosphate/insulin-like growth factor II receptor. A consensus casein kinase II site followed by 2 leucines near the carboxyl terminus is important for intracellular targeting of lysosomal enzymes. *J. Biol. Chem.* **268**, 22338-22346.

Christoforidis, S., McBride, H. M., Burgoyne, R. D. and Zerial, M. (1999). The Rab5 effector EEA1 is a core component of endosome docking. *Nature* **397**, 621-625.

Dittmer, F., Hafner, A., Ulbrich, E. J., Moritz, J. D., Schmidt, P., Schmahl, W., Pohlmann, R. and von Figura, K. (1998). I-cell disease-like phenotype in mice deficient in mannose-6-phosphate receptors. *Transgenic Res.* **7**, 473-483.

Doray, B. and Kornfeld, S. (2001). γ Subunit of the AP-1 adaptor complex binds clathrin: implications for cooperative binding in coated vesicle assembly. *Mol. Biol. Cell* **12**, 1925-1935.

Goldstein, J. L., Basu, S. K. and Brown, M. S. (1983). Receptor-mediated endocytosis of low-density lipoprotein in cultured cells. *Methods Enzymol.* **98**, 241-260.

Griffiths, J. (1993). Fine structure immunocytochemistry. Springer Verlag, Berlin.

Heilker, R., Spiess, M. and Crottet, P. (1999). Recognition of sorting signals by clathrin adaptors. *BioEssays* **21**, 558-567.

Hemer, F., Körner, C. and Braulke, T. (1993). Phosphorylation of the human 46-kDa mannose 6-phosphate receptor in the cytoplasmic domain at serine 56. *J. Biol. Chem.* **268**, 17108-17113.

Hille-Rehfeld, A. (1995). Mannose 6-phosphate receptors in sorting and transport of lysosomal enzymes. *Biochim. Biophys. Acta* **1241**, 177-194.

Hirst, J. and Robinson, M. (1998). Clathrin and adaptors. *Biochim Biophys Acta* **1404**, 173-193.

Johnson, K. F. and Kornfeld, S. (1992). The cytoplasmic tail of the mannose 6-phosphate/insulin-like growth factor-II receptor has two signals for lysosomal enzyme sorting in the Golgi. *J. Cell Biol.* **119**, 249-257.

Kang, J. X., Li, Y. and Leaf, A. (1997). Mannose-6-phosphate/insulin-like growth factor-II receptor is a receptor for retinoic acid. *Proc. Natl. Acad. Sci. USA* **94**, 13671-13676.

Kirchhausen, T. (1999). Adaptors for clathrin-mediated traffic. *Annu. Rev. Cell Dev. Biol.* **15**, 705-732.

Klumperman, J., Hille, A., Veenendaal, T., Oorschot, V., Stoorvogel, W., von Figura, K. and Geuze, H. J. (1993). Differences in the endosomal distributions of the two mannose-6-phosphate receptors. *J. Cell Biol.* **121**, 997-1010.

Kobayashi, T., Stang, E., Fang, K. S., de Moerloose, P., Parton, R. G. and Gruenberg, J. (1998). A lipid associated with the antiphospholipid syndrome regulates endosome structure and function. *Nature* **392**, 193-197.

Kornfeld, S. (1992). Structure and function of the mannose 6-phosphate/insulinlike growth factor II receptors. *Ann. Rev. Biochem.* **61**, 307-330.

Lamaze, C. and Schmid, S. L. (1995). Recruitment of epidermal growth factor receptors into coated pits requires their activated tyrosine kinase. *J. Cell Biol.* **129**, 47-54.

Ludwig, T., Eggenschwiler, J., Fisher, P., D'Ercole, A. J., Davenport, M. L. and Efstratiadis, A. (1996). Mouse mutants lacking the type 2 IGF receptor (IGF2R) are rescued from perinatal lethality in Igf2 and Igf1r null backgrounds. *Dev. Biol.* **177**, 517-535.

Méresse, S. and Hoflack, B. (1993). Phosphorylation of the cation-independent mannose-6-phosphate receptor is closely associated with its exit from the trans-Golgi network. *J. Cell Biol.* **120**, 67-75.

Meyer, C., Zizioli, D., Lausmann, S., Eskelinen, E. L., Hamann, J., Saftig, P., von Figura, K. and Schu, P. (2000). μ1A adaptin-deficient mice: lethality, loss of AP-1 binding and rerouting of mannose 6-phosphate receptors. *EMBO J.* **19**, 2193-2203.

Molloy, S. S., Anderson, E. D., Jean, F. and Thomas, G. (1999). Bi-cycling the furin pathway: from TGN localization to pathogen activation and embryogenesis. *Trends Cell Biol.* **9**, 28-35.

Motyka, B., Korbutt, G., Pinkoski, M. J., Heibein, J. A., Caputo, A., Hobman, M., Barry, M., Shostak, I., Sawchuk, T., Holmes, C. F. B., Gauldie, J. and Bleackley, R. C. (2000). Mannose 6-phosphate/Insulin-like growth factor II receptor is a death receptor for Granzyme B during cytotoxic T cell–induced apoptosis. *Cell* **103**, 491-500.

Nykjaer, A., Christensen, E. I., Vorum, H., Hager, H., Petersen, C. M., Røigaard, H., Min, H. Y., Vilhardt, F., Møller, L. B., Kornfeld, S. and Gliemann, J. (1998). Mannose 6-phosphate/insulin-like growth factor-II receptor targets the urokinase receptor to lysosomes via a novel binding interaction. *J. Cell Biol.* **141**, 815-828.

Ohno, H., Tomemori, T., Nakatsu, F., Okazaki, Y., Aguilar, R. C., Fölsch, H., Mellman, I., Saito, T., Shirasawa, T. and Bonifacino, J. S. (1999). μ1B, a novel adaptor medium chain expressed in polarized epithelial cells. *FEBS Lett.* **449**, 215-220.

Schäfer, W., Stroh, A., Berghofer, S., Seiler, J., Vey, M., Kruse, M. L., Kern, H. F., Klenk, H. D. and Garten, W. (1995). Two independent targeting signals in the cytoplasmic domain determine trans-Golgi network localization and endosomal trafficking of the proprotein convertase furin. *EMBO J.* **14**, 2424-2435.

Schmid, S. L. (1997) Clathrin-coated vesicle formation and protein sorting: an integrated process. *Annu. Rev. Biochem.* **66**, 511-548.

Stoorvogel, W., Geuze, H. J., Griffith, J. M., Schwartz, A. L. and Strous, G. J. (1989). Relations between the intracellular pathways of the receptors for transferrin, asialoglycoprotein, and mannose 6-phosphate in human hepatoma cells. *J. Cell Biol.* **108**, 2137-2148.

Stroh, A., Schäfer, W., Berghofer, S., Eickmann, M., Teuchert, M., Burger, I., Klenk, H. D. and Garten, W. (1999). A mono phenylalanine-based motif (F790) and a leucine-dependent motif (LI760) mediate internalization of furin. *Eur. J. Cell Biol.* **78**, 151-160.

Teuchert, M., Berghofer, S., Klenk, H. D. and Garten, W. (1999). Recycling of furin from the plasma membrane. Functional importance of the cytoplasmic tail sorting signals and interaction with the AP-2 adaptor medium chain subunit. *J. Biol. Chem.* **274**, 36781-36789.

Wiley, H. S., Herbst, J. J., Walsh, B. J., Lauffenburger, D. A., Rosenfeld, M. G. and Gill, G. N. (1991). The role of tyrosine kinase activity in endocytosis, compartmentation, and down-regulation of the epidermal growth factor receptor. *J. Biol. Chem.* **266**, 11083-11094.

York, S. J., Arneson, L. S., Gregory, W. T., Dahms, N. M. and Kornfeld, S. (1999). The rate of internalization of the mannose 6-phosphate/insulin-like growth factor II receptor is enhanced by multivalent ligand binding. *J. Biol. Chem.* **274**, 1164-1171.